

# A Method of Timbre-Shape Synthesis Based On Summation of Spherical Curves

Lance Putnam

Department of Architecture, Design and Media Technology

Aalborg University

Aalborg, Denmark

lp@create.aau.dk

## ABSTRACT

It is well-known that there is a rich correspondence between sound and visual curves, perhaps most widely explored through direct input of sound into an oscilloscope. However, there have been relatively few proposals on how to translate sound into three-dimensional curves. We present a novel method for simultaneous production of sonic tones and graphical curves based on additive synthesis of spherical curves. The spherical curves are generated from a sequence of elemental 3D rotations, similar to a Euler rotation. We show that this method can produce many important two- and three-dimensional curves directly from sine waves and thus provide a basic language for exploring timbre-shape relationships.

## 1. INTRODUCTION

It has long been known that there is a direct, yet fertile correspondence between sound and visual curves. The most well-known demonstrations of this include Young's visualization of the transverse orbits of vibrating strings [1], Wheatstone's vibrating rod "kaleidophone" [2], and Lissajous' light reflections off of tuning forks [3]. Most of these early experiments demonstrate that simple harmonic motions are capable of producing a seemingly endless variety of rich, complicated curves. Many artists have created visualizations of sound through *oscillography* [4], the direct mapping of two channels of sound into the x and y inputs of an oscilloscope. Most of the earlier oscilloscope works used the visual output only [5, 6, 7], but more recent works [8, 9] also present the sound used to generate the visuals.

While it is well-known that one can directly map sound pressure to curves in two dimensions and obtain interesting results, there has been little work on how to extend this to three dimensions. Perhaps the most straightforward approach is to extend the idea of oscillography by adding a third channel of sound and mapping it to the z dimension. However, the question becomes how to do this in a non-arbitrary way. Monro and Pressing [10] propose the technique of embedding where all sound channels are

derived from delayed copies of a single source. While elegant in its generality and simplicity, the choice of delay is not straightforward and many of the resulting figures, especially in three dimensions, have a box-like appearance. Also, it is not obvious how one would produce canonical shapes, like a sphere or cone, using embedding. Glassner's shape synthesizer [11] can produce a wide variety of shapes through its "vector-controlled" data flow paradigm which is inspired by voltage-controlled modular sound synthesizers. Here, the fundamental data type is a 3-vector and the modules perform scaling, rotation, translation, and other spatial transformations. While the vector-controlled shape synthesizer is very flexible, it does not produce sound nor suggest a concrete synthesis method as a starting point. The gyroscope has also been used to create 3D curves of light [12], however these curves are limited to the surface of a sphere.

In this paper, we present a novel geometric method for producing a large variety of tones and three-dimensional curves simultaneously from one equation. The method consists of two main parts: (1) generation of curves on a sphere and (2) adding together two or more of these spherical curves to produce non-spherical curves. The spherical curves are generated by rotating a point through a chain of several elemental rotations, similar to an Euler rotation, and allowing the rotation angles to vary linearly over time to produce a curve. This method can produce a wide variety of canonical shapes and rich tones and thus can serve as a useful starting point for synthesizing audiovisual forms at the level of timbre-shape [13]. Alternatively (or in addition), this method can be used to compose complex spatial trajectories that can be used, for example, for movement of sounds and/or graphical objects or for wave terrain synthesis [14].

## 2. MATHEMATICAL BACKGROUND

A well-known technique for mapping sound into visual patterns is through a method first demonstrated by French mathematician Jules Antoine Lissajous [3]. In his experiment, light was reflected off of two mirrors attached to vibrating tuning forks positioned 90° from one another. The resulting figures are described by the parametric equation

$$\begin{bmatrix} x(t) \\ y(t) \end{bmatrix} = \begin{bmatrix} \cos(\omega_1 t + \theta_1) \\ \cos(\omega_2 t + \theta_2) \end{bmatrix} \quad (1)$$

where  $\omega_k$  and  $\theta_k$  are the frequencies and initial phases of two sinusoids. The frequencies and phases of each sinu-

soid impact the shape of the resulting curve. A Lissajous curve is an orthographic projection of a sinusoidal curve on the surface of a cylinder. Such a cylindrical sinusoid can be given in cylindrical coordinates with the parametric equation

$$\begin{bmatrix} \rho(t) \\ \phi(t) \\ z(t) \end{bmatrix} = \begin{bmatrix} 1 \\ \omega_1 t + \theta_1 \\ \cos(\omega_2 t + \theta_2) \end{bmatrix} \quad (2)$$

where  $\rho$  is the radius,  $\phi$  is the angle parallel to the  $xy$ -plane and  $z$  is the distance from the  $xy$ -plane. If we convert (2) to Cartesian coordinates, we obtain

$$\begin{bmatrix} x(t) \\ y(t) \\ z(t) \end{bmatrix} = \begin{bmatrix} \cos(\omega_1 t + \theta_1) \\ \sin(\omega_1 t + \theta_1) \\ \cos(\omega_2 t + \theta_2) \end{bmatrix}. \quad (3)$$

The projection of this curve onto the  $xz$ -plane is clearly the Lissajous curve given by (1). While the family of Lissajous curves is quite varied, due to the nature of their embedding in cylindrical space, they exhibit limited degrees of symmetry having a box-like appearance and tend to be more dense near the edges of the figure.

Another type of curve, called the rose or rhodonea curve [15], can also be produced directly from sine waves. However, unlike the Lissajous curve, it offers control over the cyclic symmetry of the figure. A rose curve can be described parametrically as

$$\begin{bmatrix} x(t) \\ y(t) \end{bmatrix} = \begin{bmatrix} \cos(\omega_1 t + \theta_1) + \cos(\omega_2 t + \theta_2) \\ \sin(\omega_1 t + \theta_1) + \sin(\omega_2 t + \theta_2) \end{bmatrix} \quad (4)$$

where  $\omega_k$  are frequencies in radians/second and  $\theta_k$  are initial phases. If the two frequencies can be expressed as a simple integer ratio  $a : b$ , then the degree of cyclic symmetry of the figure is  $|a - b|$ .

Just as Lissajous curves are two-dimensional projections of a curve on a cylinder, the rose curve can be shown [16] to be a projection of a special type of curve on a sphere called a Clelia curve [15]. A Clelia curve is given by

$$\begin{bmatrix} x(t) \\ y(t) \\ z(t) \end{bmatrix} = \begin{bmatrix} \cos(\omega_1 t + \theta_1) \sin(\omega_2 t + \theta_2) \\ \sin(\omega_1 t + \theta_1) \sin(\omega_2 t + \theta_2) \\ \cos(\omega_2 t + \theta_2) \end{bmatrix} \quad (5)$$

where  $\omega_k$  are frequencies in radians/second and  $\theta_k$  are initial phases. The next section describes how we extend the Clelia curve to produce more complex spherical curves.

### 3. EULER ROTATIONS AND BEYOND

One of the interesting aspects of the Clelia curve is that its equation is identical to a spherical to Cartesian coordinate mapping—the only difference being the former describes uniform rotational motion whereas the latter describes only a mapping of position. Additionally, the spherical to Cartesian mapping can be decomposed into two elemental intrinsic rotations. This suggests that we can extend the Clelia curve through additional rotations around different axes.

Given a coordinate frame with local axes designated  $X, Y, Z$ , a Clelia curve is the path that the  $Z$ -axis of the coordinate frame traces out undergoing a rotation on its

$XY$ -plane followed by a rotation on its  $ZX$ -plane. Rotations around the  $X, Y$ , and  $Z$  axes are given, respectively, by the transformation matrices

$$\begin{aligned} R_X(\theta_k) &= \begin{bmatrix} 1 & 0 & 0 \\ 0 & c_k & -s_k \\ 0 & s_k & c_k \end{bmatrix} \\ R_Y(\theta_k) &= \begin{bmatrix} c_k & 0 & s_k \\ 0 & 1 & 0 \\ -s_k & 0 & c_k \end{bmatrix} \\ R_Z(\theta_k) &= \begin{bmatrix} c_k & -s_k & 0 \\ s_k & c_k & 0 \\ 0 & 0 & 1 \end{bmatrix} \end{aligned} \quad (6)$$

where, for brevity, we substitute  $c_k = \cos(\theta_k)$  and  $s_k = \sin(\theta_k)$ . If we perform the multiplication  $R_Z(\theta_1)R_Y(\theta_2)$ , we find that the position of the coordinate frame's  $Z$ -axis is

$$\begin{bmatrix} x(\theta_1, \theta_2) \\ y(\theta_1, \theta_2) \\ z(\theta_1, \theta_2) \end{bmatrix} = \begin{bmatrix} c_1 s_2 \\ s_1 s_2 \\ c_2 \end{bmatrix} \quad (7)$$

which has the same form as (5). We can extend this to a  $ZYX$  Euler (or Tait-Bryan) rotation by adding a third rotation around the  $X$ -axis, thus obtaining  $R_Z(\theta_1)R_Y(\theta_2)R_X(\theta_3)$ . The  $Z$ -axis now has a position given by

$$\begin{bmatrix} x(\theta_1, \theta_2, \theta_3) \\ y(\theta_1, \theta_2, \theta_3) \\ z(\theta_1, \theta_2, \theta_3) \end{bmatrix} = \begin{bmatrix} c_1 s_2 c_3 + s_1 s_3 \\ s_1 s_2 c_3 - c_1 s_3 \\ c_2 c_3 \end{bmatrix}. \quad (8)$$

The reason to choose  $ZYX$  instead of  $ZYZ$  is so that the third rotation actually moves the  $Z$ -axis. Finally, we add one more rotation along the  $Y$ -axis which can be helpful as a shape changing parameter. The final sequence of rotations becomes  $R_Z(\theta_1)R_Y(\theta_2)R_X(\theta_3)R_Y(\theta_4)$  with the  $Z$ -axis position given by

$$\begin{bmatrix} x(\theta_1, \theta_2, \theta_3, \theta_4) \\ y(\theta_1, \theta_2, \theta_3, \theta_4) \\ z(\theta_1, \theta_2, \theta_3, \theta_4) \end{bmatrix} = \begin{bmatrix} (c_1 s_2 c_3 + s_1 s_3)c_4 + c_1 c_2 s_4 \\ (s_1 s_2 c_3 - c_1 s_3)c_4 + s_1 c_2 s_4 \\ c_2 c_3 c_4 - s_2 s_4 \end{bmatrix}. \quad (9)$$

This final form is the most general as it produces (7) and (8) when  $\theta_3 = \theta_4 = 0$  and  $\theta_4 = 0$ , respectively.

### 4. GENERATION OF SOUND AND GRAPHICS

To produce sound waveforms and curves from (9), we can perform the substitution  $\theta_k \rightarrow \omega_k t + \theta_k$  where  $t$  is time, in seconds, and  $\omega_k$  is the frequency, in Hz, of the  $k^{th}$  elemental rotation. Fundamentally, we therefore have 9 parametric controls for each spherical curve—a frequency and phase for each of the four elemental rotations and a global scaling/gain factor. The cosine and sine terms can be generated accurately and efficiently using wavetables [17] or recursive complex multiplication [18]. The phase accumulators or complex multiplications require, at a minimum, double-precision floating-point arithmetic to obtain an acceptable level of phase coherency between the elemental rotations over time. This is important as, visually, the curve shapes are highly sensitive to the phases.

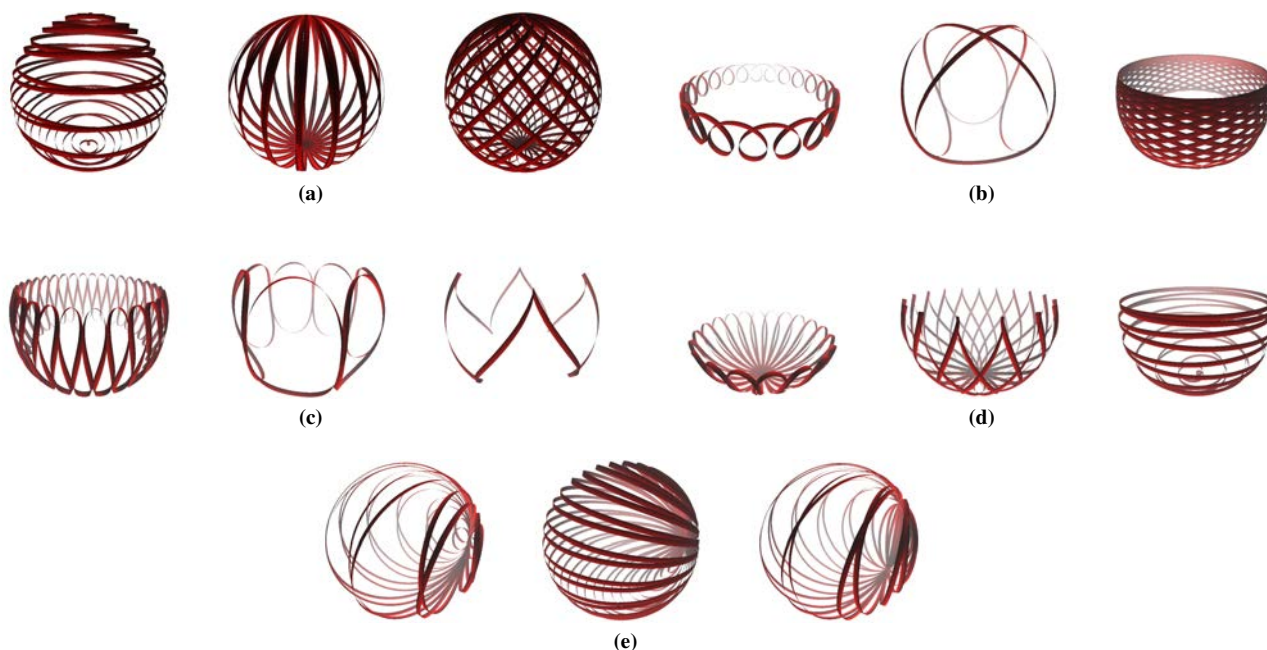


**Figure 1.** Some basic types of spherical curves: (a) Clelia curve, (b) spherical trochoid, (c) satellite curve, (d) spherical rose, and (e) warped Clelia curve.

Sound can be produced by using the  $x, z$  or  $y, z$  coordinates of the  $Z$  axis. The  $x$  and  $y$  coordinates have the potential to be rich in sine waves since they contain several trigonometric products; in terms of synthesis this can be viewed as recursive ring modulation. Each product of sinusoids produces a sum of sinusoids whose frequencies are the sum and difference of the sinusoid factor frequencies. A product of four sinusoids can produce a sum of eight sinusoids, for instance. Thus, referring to (9), the  $x$  (or  $y$ ) and  $z$  components can produce a maximum of 16 and 6 unique sine waves, respectively, leading to potentially rich tones. The  $x$  and  $y$  components can be played out separately in the left and right channels to produce complex stereo phasing effects.

Graphically, it may be desirable to avoid overdrawing the curve to reduce visual clutter and/or to improve rendering efficiency. To do this, we only render enough vertices to draw one period of the curve. Given a fundamental frequency  $f$  and audio sample rate  $f_s$ , the number of vertices in one period is  $N = f_s/f$ . Optionally, we can simulate a frame blurring effect by intentionally overdrawing the curve using some integer multiple of  $N$ .

## 5. DISCUSSION OF PATTERNS

In this section, we present and discuss some of the patterns that can be produced from the intrinsic  $ZYXY$  rotation given in (9). For brevity, we use  $\{k, \theta\}_B$  to represent a rotation of  $2\pi(fkt + \theta)$  radians around axis  $B$  where  $f$  is some fundamental frequency, in Hz, and  $t$  is time, in seconds. If  $\theta$  is not given, it is assumed to be 0.

A general principle to note is that by selecting harmonically-related frequencies throughout, we obtain a stable, yet monotonous, timbre and shape. To make the

timbre and shape more lively and evolve over time, we can choose slightly inharmonic frequencies.

### 5.1 Spherical Curves

First, the spherical patterns are discussed. Examples are shown in Figure 1. A Clelia curve is given by  $\{a\}_Z\{b\}_Y$ . When  $a \ll b$  the pattern is sectoral “slicing” the sphere, when  $a \gg b$  the pattern is zonal producing “stacks”, and when  $a \approx b$  the pattern is tesseral. Sectoral motions follow great circles moving mostly *through* the poles, zonal motions move predominantly *around* the poles, and tesseral motions move equally around and through the poles. Visually, surfaces generated from tesseral curves tend to have a more solid appearance. Using slightly inharmonic frequencies causes the curve to spin around the  $z$  axis. We can move the poles of the Clelia curve symmetrically along a great circle with  $\{a\}_Z\{b\}_Y\{a\}_X\{0, \theta\}_Y$  where  $\theta$  controls the amount of displacement of the poles. A spherical trochoid [19] is produced with  $\{a\}_Z\{b\}_Y\{0, \theta\}_X$  where  $\theta$  controls the spread of the curve from the equator. A satellite curve<sup>1</sup> has the equation  $\{a\}_Z\{0, \theta\}_Y\{b\}_X$ . This curve is similar to the spherical trochoid except that it has glide-reflection symmetry with respect to the equator. It is possible to create interesting time-varying patterns with the spherical trochoid and satellite curve by replacing the zero-valued frequency with a low (sub-audio) frequency in the range of approximately 0-5 Hz. Lastly, a spherical rose curve can be produced from  $\{a\}_Z\{0, \theta\}_Y\{b\}_X\{0, \theta\}_Y$  where  $\theta$  controls the degree to which the curve covers the sphere. Again, replacing the zero-valued frequencies with low frequencies produces a variety of intriguing time-varying shapes and timbres.

<sup>1</sup> <http://www.mathcurve.com/courbes3d/satellite/satellite.shtml>

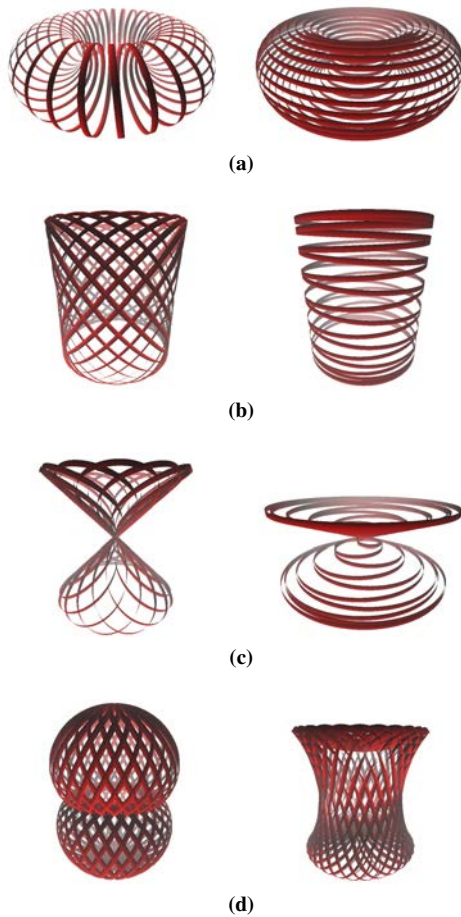


**Figure 2.** Non-spherical shapes made from a sum of two Clelia curves: (a) toroidal sinusoid, (b) cylindrical sinusoid, (c) conical sinusoid, and (d) centered trochoid surfaces of revolution generated from a nephroid (left) and astroid (right)

## 5.2 Non-spherical Curves

While many types of curves can be produced on a sphere, we can also generate curves with different surface structure by adding spherical curves together. Here, we present some of the patterns that can be produced from sums of Clelia curves. A toroidal sinusoid is generated from  $r_{min}\{a\}_Z\{b\}_Y + r_{maj}\{a\}_Z\{0, \frac{1}{4}\}_Y$  where  $r_{min}$  and  $r_{maj}$  are the minor and major radii. Similar to a Clelia curve, when  $a \ll b$  we obtain a “sliced” torus and when  $a \gg b$  the curve forms “stacks”. It is possible to generate sinusoidal patterns on a cylinder, double cone, and sphere with  $\{a\}_Z\{b\}_Y + \{a, \theta\}_Z\{b, \frac{1}{4}\}_Y$  where  $\theta = 0$  is a sphere,  $\theta = \frac{1}{4}, \frac{3}{4}$  is a cylinder, and  $\theta = \frac{1}{2}$  is a double cone. The cylindrical sinusoid, when projected on a plane intersecting the  $z$ -axis, produces a Lissajous curve. Finally, we can obtain centered trochoid surfaces of revolution with  $\{m\}_Z\{n, \phi\}_Y + A\{am, \theta\}_Z\{bn\}_Y$  where  $\phi$  adjusts the revolution axis and  $\theta$  controls whether the base curve is inward or outward looping. Examples of these non-spherical curves are shown in Figure 2.

Figure 3 presents some shapes with more complicated



(a)  $\{10\}_Z\{11\}_Y\{12\}_X\{55\}_Y$



(b)  $\{31\}_Z\{30\}_Y\{29\}_X\{29\}_Y + \{31\}_Z\{30, \frac{1}{4}\}_Y\{29, \frac{1}{4}\}_X\{29\}_Y$

**Figure 3.** More complex (a) spherical and (b) non-spherical shapes with less symmetry apparent.

patterns. The curves still have symmetry, but it can be difficult to see depending on the orientation the curve is viewed at.

## 5.3 Motion Trajectories and Ornamentation

As mentioned previously, the spherical curves can also be used to create trajectories in space. The patterns discussed above remain, for the most part, fixated at the origin. To make them move in space, we can simply add one or more additional spherical curves whose frequencies are all at sub-audio rates, for instance, in the range of 0-5 Hz. For listening, the low-frequency components can either be filtered out using a DC blocker or can be split out beforehand from the audio and sent as coordinates to a separate sound spatialization process. Typically, the trajectory curve will be much lower in frequency and higher in amplitude than the base curve. Figure 4a shows the sum of a Clelia curve given by  $\frac{1}{3}\{1\}_z\{8\}_Y$  and a trajectory given by  $\{\frac{1}{100}\}_z\{\frac{8}{100}\}_Y$ . The history is exaggerated somewhat to show the trajectory of the curve, but also shows how the trajectory will unavoidably distort the base shape.

One can add ornamentation to a base curve by adding one or more spherical curves with a much higher frequency and lower amplitude. Due to the high frequencies, it might be desirable to exclude the ornamenting curve from the audio signal to avoid aliasing. Figure 4b shows a Clelia curve  $\{1\}_z\{8\}_Y$  combined with an ornamenting Clelia curve  $\frac{1}{10}\{100\}_z\{800\}_Y$ .

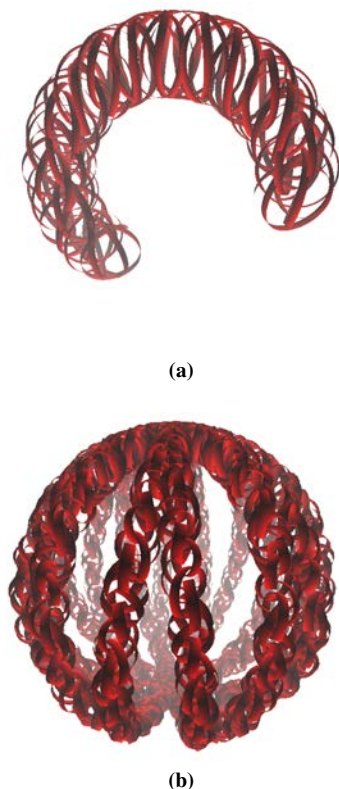


**Figure 4.** Adding low-frequency spherical curves permits the construction of trajectories in space. Figure (a) is the sum of a Clelia curve and a higher-amplitude, lower-frequency circular motion. Curves can be ornamented by adding high-frequency curves to them. Figure (b) is a sum of a Clelia curve with a lower-amplitude, higher-frequency Clelia curve.

## 6. CONCLUSION

We have shown a promising new method of generating three-dimensional curves from sine waves via sequences of rotation matrices. Since each rotation stage is driven by an independent complex sinusoid, it is possible to create a multitude of spherical curves and rich sonic tones. Adding two spherical curves together already shows great promise for producing curves with non-spherical shapes such as torii, double cones, and more general surfaces of revolution. Although not investigated, sums of three or more spherical curves will almost certainly extend the reach of possible shapes and timbres. While the presented method shows great promise for simultaneous timbre-shape synthesis, a couple issues remain. First, many of the shapes observed so far tend to have a dominant axis of revolution and thus limited symmetry. It remains an open question whether this method is sufficient for producing curves with more general point group symmetries. Second, phase has a much more significant effect on the resulting visual forms than on the sound. This issue could potentially be addressed by using a sound mapping based on a more visually salient property of the curve, such as its curvature.

## 7. REFERENCES

- [1] T. Young, “Outlines of experiments and inquiries respecting sound and light,” *Philosophical Transactions of the Royal Society of London*, vol. 90, pp. 106–150, 1800.
- [2] C. Wheatstone, “Description of the kaleidophone, or phonic kaleidoscope; a new philosophical toy, for the illustration of several interesting and amusing acoustical and optical phenomena,” *The Quarterly Journal of Science, Literature and Art*, vol. 23, pp. 344–351, 1827.
- [3] J. A. Lissajous, “Mémoire sur l’étude optique des mouvements vibratoires,” *Annales de Chimie et de Physique*, vol. 51, pp. 147–231, 1857.
- [4] H. W. Franke, *Computer Graphics - Computer Art*, second, revised and enlarged ed. Springer-Verlag, 1985.
- [5] B. Laposky, “Electronic abstraction: A new approach to design,” Exhibition Catalogue, Sanford Museum, Cherokee, Iowa, 1953.
- [6] N.-J. Paik and Y. Jud, *Beatles Electroniques*, 1969.
- [7] A. Vitkine, “Photographic and electronically generated images,” *Leonardo*, vol. 19, no. 4, pp. 305–309, 1986.
- [8] R. Fox, *Backscatter*, 2005.
- [9] A. Callejo, *Sincrotró 3238*, 2007.
- [10] G. Monro and J. Pressing, “Sound visualization using embedding: The art and science of auditory autocorrelation,” *Computer Music Journal*, vol. 22, no. 2, pp. 20–34, 1998.
- [11] A. S. Glassner, “A shape synthesizer,” *IEEE Computer Graphics and Applications*, vol. 17, no. 3, pp. 40–51, 1997.
- [12] K. Rutherford, “The emergence of gyroscopic spherical curves,” Accessed from <http://www.vacuumphysics.net/?q=the-emergence-of-gyroscopic-spherical-curves>, 2007.
- [13] A. Abbado, “Perceptual correspondences of abstract animation and synthetic sound,” *Leonardo. Supplemental Issue*, vol. 1, pp. 3–5, 1988. [Online]. Available: <http://www.jstor.org/stable/1557901>
- [14] H. Mikelson, *The Csound Book: Perspectives in Software Synthesis, Sound Design, Signal Processing, and Programming*. MIT Press, 2000, ch. Terrain Mapping Synthesis.
- [15] G. Grandi, *Flores Geometrici Ex Rhodonearum Et Cloeliarum Curvarum Descriptionibus Resultantes*. Kessinger Publishing, LLC, 1728.
- [16] G. Lucarelli, R. Santamaria, S. Troisi, and L. Turturici, “Flowers and satellites,” *Journal of Navigation*, vol. 44, no. 1, pp. 122–126, 1991.

- [17] J. Tierney, C. M. Rader, and B. Gold, "A digital frequency generator," *IEEE Transactions on Audio and Electroacoustics*, vol. AU-19, no. 1, pp. 48–57, March 1971.
- [18] J. W. Gordon and J. O. Smith, "A sine generation algorithm for VLSI applications," in *Proceedings of the 1985 International Computer Music Conference*, 1985, pp. 165–168.
- [19] H. M. Jeffery, "On spherical cycloidal and trochoidal curves," *The Quarterly Journal of Pure and Applied Mathematics*, vol. 19, pp. 44–66, 1883.